Integrative Biology

Accepted Manuscript

ROYAL SOCIETY OF CHEMISTRY

www.rsc.org/ibiology

Fluctuations and Synchrony of RNA Synthesis in Nucleoli

Artem Pliss[a]†, Andrey N. Kuzmin[a]†, Aliaksandr V. Kachynski[a#], Alexander Baev[a], Ronald Berezney[b] and Paras N. Prasad[a,c*]

a Institute for Lasers, Photonics and Biophotonics and the Department of Chemistry, University at Buffalo, the State University of New York, Buffalo, NY 14260

b Department of Biological Sciences, University at Buffalo, the State University of New York, Buffalo, NY 14260

c Department of Chemistry, Korea University, Seoul 136-701, Korea

Present Address: Aliaksandr Kachynski, Beckman Coulter Inc., Life Science Division, 4862 Innovation Drive, Fort Collins, CO 80525

*Correspondence to: pnprasad@acsu.buffalo.edu

†These authors contributed equally

KEYWORDS *(ribosomal RNA; ribosome biogenesis; nucleolus; fluctuations of gene expression; Raman spectroscopy)*

Received (in XXX, XXX) Xth XXXXXXXXX 20XX, Accepted Xth XXXXXXXXX 20XX

DOI: 10.1039/b000000x

ABSTRACT: Ribosomal RNA (rRNA) sequences are synthesized at exceptionally high rates and, together with ribosomal proteins (r-proteins), are utilized as building blocks for assembly of pre-ribosomal particles. Although it is widely acknowledged that a tight regulation and coordination of rRNA and r-proteins production are fundamentally important for maintenance of cellular homeostasis, still little is known about the real-time kinetics of these ribosome components synthesis in individual cells. In this communication we introduce a label-free MicroRaman spectrometric approach for monitoring of rRNA synthesis in live cultured cells. Remarkably high and rapid fluctuations of rRNA production rates were revealed by this technique. Strikingly, the changes in the rRNA output were synchronous for ribosomal genes located in separate nucleoli of the same cell. Our findings call for development of new concepts to elucidate coordination of ribosomal components production. In this regard, numerical modeling further demonstrated that the production of rRNA and r-proteins can be coordinated, regardless of the fluctuations in rRNA synthesis. Overall, our quantitative data reveal a spectacular interplay of inherently stochastic rates of RNA synthesis and the coordination of gene expression.

INTRODUCTION

Ribosomal genes (rDNA) represent remarkably robust and attractive system for studies of gene expression. Human diploid genome contains approximately 400 identical copies of rDNA sequences which are clustered together in head-to-tail arrays on the well known chromosome positions [1]. While many rDNA clusters are transcriptionally dormant, several clusters are intensively transcribed by RNA polymerase I, giving rise to the ribosomal RNA (rRNA). The rRNA sequences are then utilized as a material for ribosomes formation. In this complex process, nascent rRNA transcripts are modified and together with multiple ribosomal proteins (r-proteins) and a short RNA sequence synthesized by the RNA polymerase III, assembled into pre-ribosomal particles, and then exported to the cytoplasm [2].

Studies of rDNA expression benefit from the location of rDNA sequences within specific compartment of the nucleolus [1a, 3]. The rDNA sequences are believed to be the only active genes in nucleoli and their expression continues throughout the interphase of the cell cycle, with the only known interruptions during the rDNA replication [1a, 4]. This greatly facilitates identification of transcription signal and data analysis. Moreover, the rRNA production is the most intense gene expression process in almost any type of cells. For instance, in the genome of HeLa cells there are about 150 transcriptionally active rDNA sequences, each simultaneously transcribed by ~ 100 RNA polymerase I units, which collectively produce up to 80% of the RNA in the cell [5].

Considering the vast expenditure of cellular resources used in ribosome formation, it is generally assumed that synthesis of r-RNA and r-proteins should be tightly coordinated to yield equimolar amounts of these ribosome components [6]. The basis for such coordination is provided through several gene regulation and signal transduction pathways [5b, 7]. At the same time, gene expression is known to be a fundamentally stochastic process, where the rates of RNA and protein synthesis fluctuate in time [8], and therefore the level of coordination is not clear [6].

Quantitative monitoring of RNA synthesis, has established two sources of stochasticity in gene expression rates. One source encompasses variations in the intracellular concentrations of biomolecules participating in the synthesis of RNA (e.g. RNA polymerases, basal transcription factors, nucleotides), which collectively cause synchronous changes in the expression rates of many genes within the same cell; such fluctuations are referred to as an extrinsic noise of gene expression [8a]. The second source of stochasticity is associated with the randomness of molecular interactions (e.g. random collisions of macromolecules can activate or deactivate promoter, modulate kinetics of RNA synthesis, processing and decay), which leads to uncorrelated variations in expression levels of identically regulated genes

located in the same cell. The latter type of stochastic changes in levels of RNA and protein synthesis is known as the intrinsic noise of gene expression [8a, 9]. Stochastic fluctuations of gene expression generate a substantial variability in regulation of housekeeping functions, differentiation, aging and response to external stimuli, even in genetically identical populations of cells [8c, d, 10]. On another hand, these fluctuations provide additional levels of control for coordination of gene networks [11]. Hence, characterization of gene expression rates is of outmost importance for understanding of complex cellular regulation.

At the same time, quantitative studies of gene activity in live cells require new experimental paradigms. In this research field, traditional cell-population averaging approaches have a limited value, as they cannot detect stochastic fluctuations in the amounts of RNA and proteins production in different cells [12] and thus, the focus of research is increasingly shifting towards single-cell models [8a, 8c, 13].

At a single cell level, probing of gene activity typically involves tethering of fluorescent reporters to either RNA or protein gene products [14]. Recently, a two-color RNA labeling approach was proposed for simultaneous monitoring of different genes and analysis of intrinsic noise in mRNAs synthesis [15]. However, fluorescence techniques are limited for studies of rDNA expression, as any tethering of rRNA with exogenous markers would likely impair formation of ribosomes and may cause cell death.

Nevertheless, limitations of conventional techniques can be overcome by non-invasive vibrational spectroscopic approaches, such as Raman spectroscopy [16]. Label-free Raman spectroscopy relies on inelastic scattering of monochromatic light irradiating the sample, when the energy of photons is being changed, either up or down, following interactions with different types of molecules. This process generates a Raman spectrum, which essentially represents a chemical fingerprint of the studied sample and allows measuring concentrations of major classes of macromolecules such as proteins, RNA, DNA, lipids, or saccharides at the site of spectra acquisition [17]. In contrast to fluorescence based techniques, no staining of nucleic acid sequences or proteins in the sample is required, as the Raman spectra are generated by interactions of light with native cellular macromolecules. Moreover, Raman spectroscopy can utilize excitation in red to near-IR spectral region, which usually does not cause any measurable phototoxicity and permits for long time monitoring of the biochemical environment in live cells.

In our communication we introduce a single cell assay, where confocal Raman microspectrometry is employed for label-free monitoring of ribosomal gene expression. With this experimental system, we accomplished real-time measurements of rRNA production at the level of single nucleoli. We discovered that rates of rRNA synthesis fluctuate in time, and characterized the magnitude and the frequency of these fluctuations. We demonstrate that fluctuations in the rDNA activity largely correspond to the extrinsic noise of gene expression [9]. Next, by numerical modeling, we analyze coordination between rRNA and r-proteins synthesis. To the best of our knowledge, this is the first quantitative analysis of rDNA expression rates at the single cell level.

RESULTS

Raman Microspectrometry Approach for Monitoring of rRNA Synthesis in Single Nucleoli

In the present communication, we introduce high resolution confocal Raman microspectroscopy to monitor the levels of rRNA production from a group of rDNA sequences located in the same nucleolus [17a, 18]. Raman microspectrometry studies were performed in cultured cells, which were incubated under physiological conditions. Identification of nucleoli does not require staining, and is easily accomplished in live cells with transmission light imaging. Cells with representative morphology and relatively large nucleoli measuring ~5 μm in diameter were selected for spectroscopic analysis. Next, the excitation laser beam was placed over the center of the nucleolus and time–lapse series of Raman spectra were acquired (Fig. 1). The obtained spectra were then analyzed by using a semi-automated Biomolecular Component Analysis (BCA) algorithm to determine the local concentrations of RNA and proteins at each time point [17a, 18]. The RNA Raman signal was assigned specifically to rRNA, as it constitutes almost the entire RNA pool in the nucleolus [1a, 3b, 19].

In the context of nucleolar function, the concentration of RNA is chiefly determined by two variables: (1) the rate at which new rRNA sequences are synthesized from all active rDNA repeats located in the same nucleolus; and (2) the rate at which rRNA sequences are removed from the nucleolus. This second variable includes both the removal of introns from pre-rRNAs as well as the export of pre-ribosomal particles, containing rRNA sequences, from the nucleolus. It is apparent, that any changes in

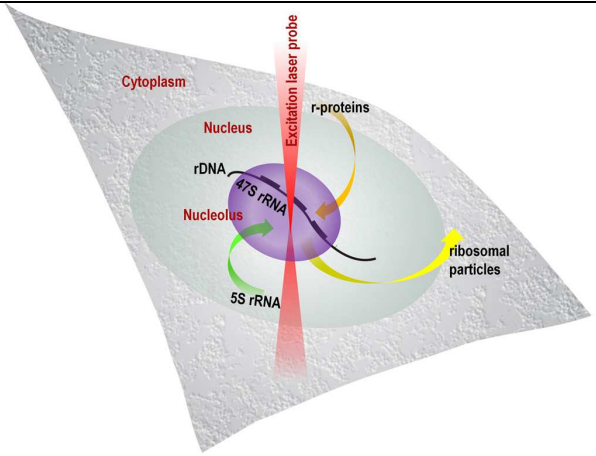

Figure 1. Schematic representation of the Raman microspectroscopy approach for monitoring of the rRNA synthesis in the nucleolus. Multiple copies of ribosomal genes (rDNA) are transcribed by RNA Polymerase I in the nucleolus, giving rise to 47S rRNA sequence. RNA Polymerase I transcripts are assembled together with 5S-RNA and ribosomal proteins (r-proteins) into pre-ribosomal particles, which are then exported to the cytoplasm. In our approach dense nucleoli are located by using a transmission light imaging. The laser beam is focused on nucleolus to excite Raman spectra, with several minute intervals. The algorithm of Biomolecular Component Analysis (BCA) yields RNA concentrations at each time point, to monitor changes in the expression rates of rDNA sequences.

the rate at which rRNA is synthesized or the rate at which it abandons the nucleolus, would produce corresponding changes of RNA concentration. Below we characterize the role of both variables on the concentration of RNA in the nucleolus and show that Raman spectroscopy enables a quantitative monitoring of rRNA synthesis.

Experimental Measurements

The output of rRNA is known to increase throughout the interphase, from G1- to G2- phase of the cell cycle. To account for cell-cycle dependent changes in the activity of rRNA synthesis, all our measurements were carried out on G1-cells [20]. To obtain cells in the G1-phase, we did not use any chemical synchronization, as it can produce artificial measurement variations in single-cell assays [21]. Instead, cell cultures were examined in transmission light, mitotic cells were identified and tracked until they completed division and entered the G1-phase of a cell cycle.

At the onset of G1-phase, multiple rDNA sequences are simultaneously activated for transcription, and discrete nucleolar domains begin to form inside the cell nucleus. Earlier, it has been estimated that complete restoration of rRNA synthesis is a gradual process consuming approximately two first hours of interphase, although the dynamics of recovery may vary in different cells [20, 22].

Raman spectroscopic monitoring of nucleolus uniquely enables quantitative measurements of the post-mitotic recovery of rRNA synthesis at the single cell level. 20-40 min after cytokinesis, the excitation laser beam was focused on nucleolus and the Raman spectra were acquired with intervals ranging from 10 - 60 min. BCA was used to determine the concentrations of RNA and proteins in the nucleoli of individual cells at each time point [18] (Fig. S1). Our analysis typically detected a sustained increase in RNA concentration in the nucleoli, from ~5 to ~30-40 mg/ml within two hours after completion of mitosis (Fig. 2A). The increase was most rapid in the first 40-60 minutes of observation, when the RNA concentration doubled every 15-20 minutes. At the second hour of the interphase recovery, the RNA concentration progressively slowed (Fig. 2A). We also found that the

concentration of the nucleolar proteins was changing in synchrony with that of RNA (Fig. 2B), from ~110 to ~160 mg/ml in the same period of G1-phase. Overall, the recovery duration of ~2h was consistent with the data obtained by conventional fluorescence imaging techniques [22b-d]. We thus concluded that the changes in the RNA and proteins concentrations reflect a post-mitotic recovery of rDNA expression in individual nucleoli.

All further studies were performed 2h - 6h from the beginning of interphase, when the nucleolar structure and rRNA synthesis are believed to be fully recovered [22b, c]. In HeLa cells this period of interphase typically corresponds to the G1-phase of the cell cycle [23]. The interval between the Raman spectroscopy measurements ranged between 3 and 20 min. A 3 min interval was chosen, because it roughly corresponds to the time required for synthesis of rRNA sequence by RNA polymerase I, and thus is more suitable for real-time quantitative analysis [5a]. Longer time intervals were selected to reduce the cumulative irradiation dose

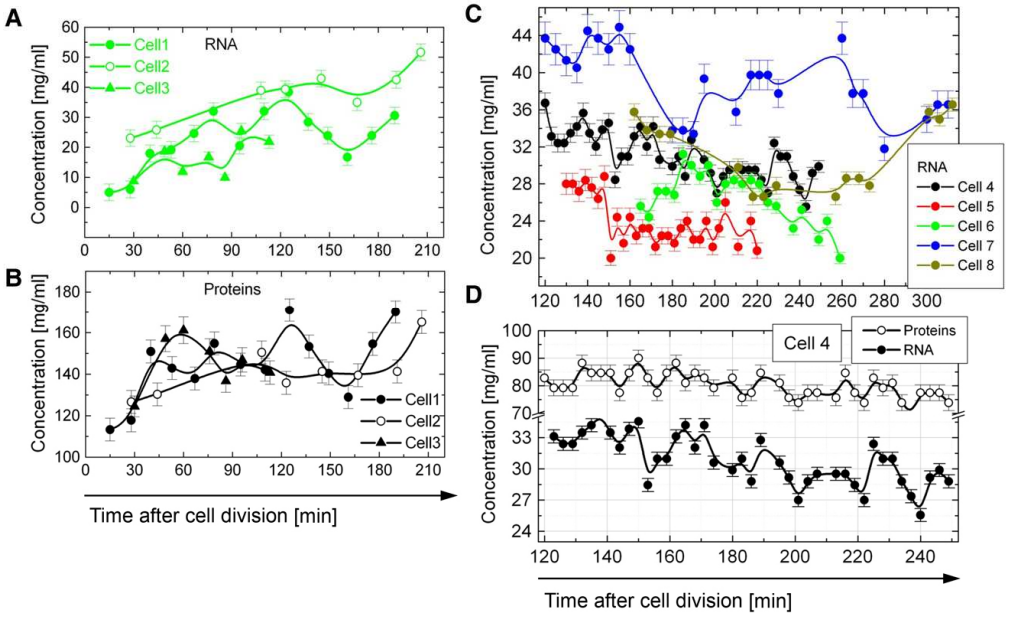

Figure 2. Monitoring of RNA synthesis in single nucleolus by Raman microspectroscopy. (A-B) Time-lapse series of Raman spectra were acquired in the nucleoli of postmitotic cells and the local concentrations of RNA and proteins at each time point were determined by the BCA spectra analysis; Chart (**A**) illustrates changes in the concentrations of nucleolar RNA during the early G1-phase progression, on example of three representative cells. Chart (**B**) shows the corresponding changes in the concentration of nucleolar proteins in the same cells. (**C-D**) Data were obtained in the cells ~2-5 hours after completion of mitosis; (**C**) Charts demonstrate the concentrations of RNA in the single nucleoli. The spectra were acquired with variable time intervals to ensure the reproducibility of the measurements. (**D**) An overlay of the nucleolar RNA and the nucleolar proteins concentration charts, obtained for cell #4 shown in (**C**). Charts on (**D**) demonstrate that changes in the concentration of RNA are accompanied by synchronous changes in the concentration of proteins.

and avoid potential cytotoxicity over the course of measurements. Measurements were performed on fifty individual cells to characterize cell-to-cell variations. Using the BCA approach, we found that molecular composition significantly varies in different nucleoli. The concentration of RNA was ranging from ~15 to ~40 mg/ml, and the concentration of proteins was in a range between ~60 and 170 mg/ml.

Strikingly, we found that the concentrations of RNA and proteins in the same nucleolus frequently fluctuate in time. The changes in nucleolar RNA and protein concentrations seem to be random, and resemble an asymmetrical oscillation pattern (Fig. 2B-D). The time period when RNA concentration was changing in the same direction, either increasing or decreasing, ranged between 5 to 20 min. Within these relatively short periods, the RNA concentration values were changing from 5 to 30% (Fig. 2C). We also observed that the concentration of proteins fluctuates synchronously with RNA, although with a lower amplitude, typically not exceeding ~15% (Fig. 2D, Fig. S2, Fig. S3). The synchrony between the changes in the RNA and protein concentrations was similar to that during the postmitotic recovery of rRNA synthesis (Fig. 2A-B, Fig. S3).

Our next goal was to identify cellular mechanisms responsible for oscillations of the RNA concentration in the nucleolus. As discussed above, the concentration of rRNA in the nucleolus can be determined by both: rates at which rRNA is synthesized and rates at which rRNA exits the nucleolus. To characterize significance of these factors, cells were treated with actinomycin D, which inhibits RNA synthesis by intercalation into DNA. The efficiency of actinomycin D action correlates with its concentration [24]. Using a low concentration of this transcription inhibitor (~0.03 μg/ml), which selectively suppresses RNA polymerase I activity over a course of several hours [24], we measured a steady and substantial reduction of the RNA signal during the drug treatment (Fig. 3A). These results confirm a correlation between the levels of rRNA synthesis and concentration of RNA in the nucleolus, and indicate that fluctuations of nucleolar RNA concentration could be caused by changes in the transcription activity of rDNA sequences.

Next, a higher concentration of actinomycin D (10 μg/ml) was applied. At this concentration, drug acts almost instantaneously, completely disrupting the synthesis of rRNA within 2 min of treatment. However, processing of already synthesized rRNA and its export from nucleolus are not inhibited by actinomycin D [25]. We considered that when the synthesis of rRNA is stalled, while processing of already synthesized rRNA as well as export of ribosomes continues, monitoring of RNA concentration can reveal the dynamics at which rRNA sequences exit the nucleolus. In response to this treatment, there was an abrupt decrease in the nucleolar RNA concentration. Within 7-12 min after the drug addition, the concentration of RNA was reduced several fold to ~5 μg/ml or lower, close to the detection threshold (Fig. 3B). This reduction was relatively uniform, although in some cells we observed minor fluctuations in the kinetics of rRNA reduction. However, the frequency and the amplitude of these fluctuations were significantly lower than in the nucleoli of untreated cells.

In another series of experiments, cells were treated with 5,6-dichloro-1-beta -D-ribofuranosylbenzimidazole (DRB), which is known to disrupt ribosome formation, through two supplementary mechanisms. First, DRB inhibits early steps in the rRNA processing and interrupts maturation of the rRNA components of ribosome [24, 26]. Second, DRB selectively inhibits the activity of RNA polymerase II, thus suppressing the synthesis of r-proteins as well as other proteins involved in ribosome formation [24]. At the same time, the RNA polymerase I activity is not sensitive to DRB, and the synthesis of rRNA precursors continues in nucleoli of the treated cells [24]. However, the kinetics RNA export from the nucleolus can become more uniform due to elimination of complex and multistage processes of ribosome formation. Nevertheless, we found that in DRB treated cells, fluctuations of the rRNA concentration continue at a similar scale as in nucleoli

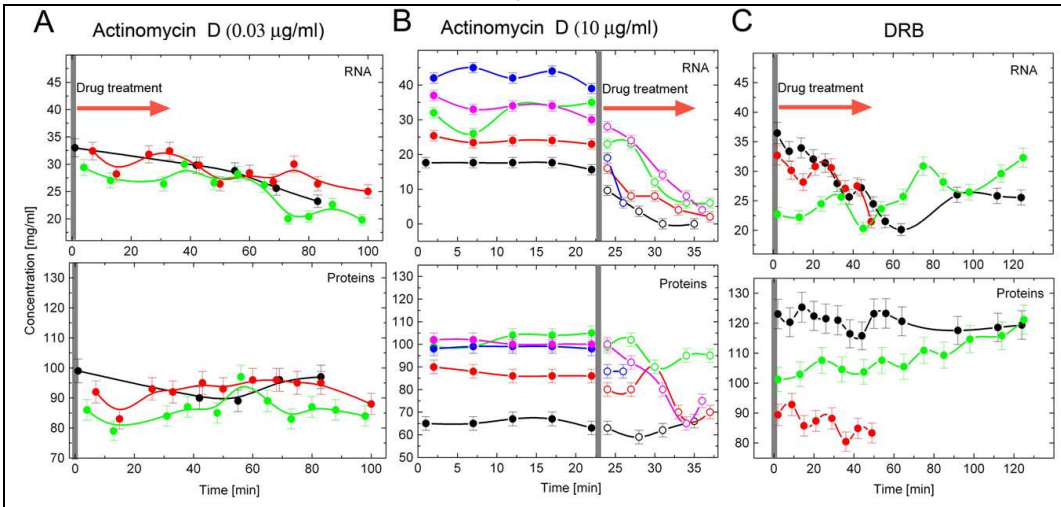

Figure 3. Inhibition of rRNA synthesis, but not rRNA processing, leads to a reduction in the nucleolar RNA concentration fluctuations. Concentrations of RNA and proteins were measured in nucleoli of the cells treated either with low concentration of actinomycin D (0.03 μg/ml) for gradual inhibition of RNA polymerase I **(A)**; high concentration of actinomycin D (10 μg/ml) for rapid inhibition of rRNA synthesis (**B**); or with DRB (50 μg/ml) for inhibition of rRNA processing and ribosome biogenesis (**C**). On the charts concentrations of RNA and proteins (mg/ml) in the nucleolus are plotted against the observation time (min). Start of the drugs treatment is marked by grey lines and arrows.

of untreated cells (Fig. 3C). These data suggest that potential variations in the kinetics of rRNA export do not significantly contribute to the generation of fluctuations of the RNA concentration in the nucleolus. Altogether, our measurements on the treated cells (Fig. 3 A-C) indicate that the fluctuations of RNA concentrations in nucleolus are largely produced by the changing activity of rRNA genes.

Next, we studied whether the fluctuations of rRNA synthesis from different copies of rDNA genes correlate in time. Typically each HeLa cell contains several nucleoli, each accommodating multiple rDNA copies [27]. As all rDNA repeats share the same regulation mechanisms, a synchronous fluctuations of the RNA synthesis rates in different nucleoli, would be an example of an extrinsic noise, caused by stochastic variations in abundance of gene-regulatory macromolecules. In contrast, an intrinsic noise would be characterized by asynchronous fluctuations of RNA output in each studied nucleolus [9].

In these experiments, we simultaneously monitored two similarly sized nucleoli located in the same cell nucleus of four representative cells. The Raman spectra were sequentially collected in each nucleolus, and the RNA concentrations in both nucleoli were calculated for each measurement time (Fig. 4). To evaluate correlation between fluctuations of RNA synthesis in different nucleoli of the same cell, we utilized Pearson coefficients (r). The Pearson coefficients characterize the strength and direction of a linear relationship between two variables on a scale from -1 to 1, where 0 corresponds to the absence of any correlation.

The Pearson coefficients were found in a positive range, varying from ~0.62 to 0.87, with an average of ~0.75, thus indicating an evident synchrony in rRNA production in different nucleoli of the same cell (Fig. 4). We further conclude that the synchronous fluctuations into different nucleoli are indicative of the extrinsic noise of gene expression [9]. At the same time, we observed periodic mismatches of rRNA concentration profiles, potentially due to intrinsic noise in expression of individual rDNA copies.

Numerical Modeling

To understand whether coordination of rRNA and r-proteins synthesis can exist despite the stochastic fluctuations in their output, we generated a numerical model based on experimentally measured rRNA concentration fluctuations. In this model, the rate of rRNA synthesis is regulated to match the supply of r-proteins in order to minimize energy expenditure for ribosome production. In our numerical modeling approach, we simulated the time evolution of rRNA concentration in the nucleolus via the continuous-time Markov birth-death process. The sign of time derivative in the master equation, determining the direction of the process (either birth or death), is a function of randomly varying protein concentrations. The birth rate equals the death rate in this approximation, so that any intrinsic noise in the production of rRNA is neglected. The extrinsic noise, i.e., fluctuations of the

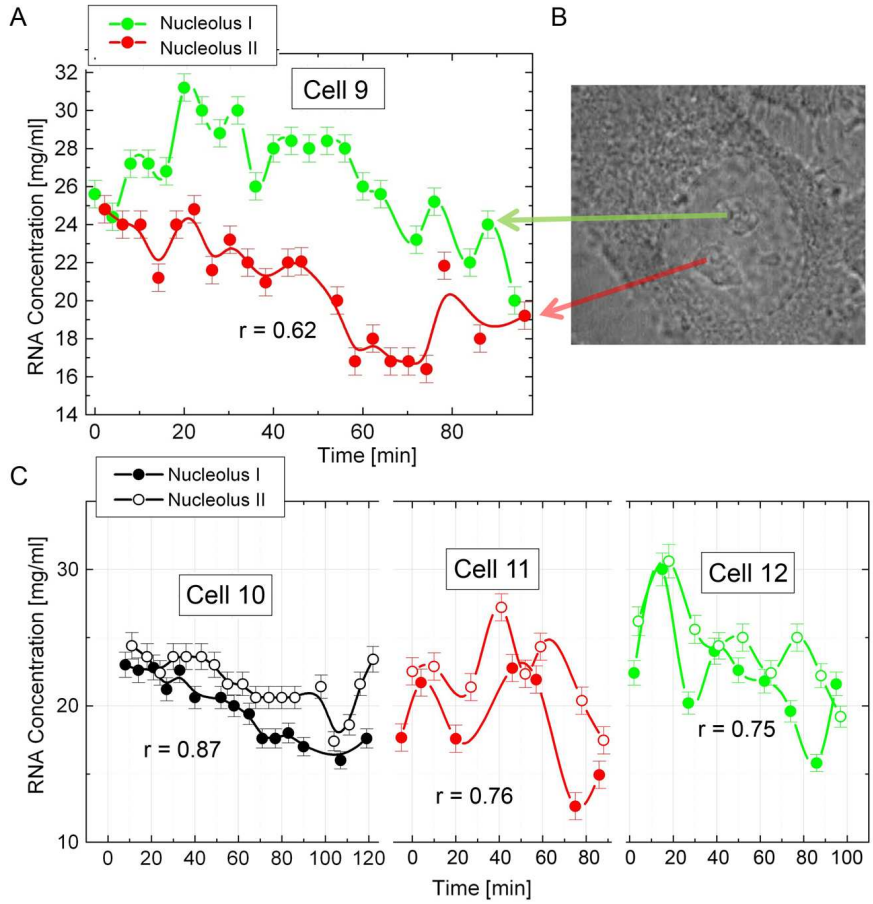

Figure 4: Fluctuations of RNA synthesis are synchronous in different nucleoli of the same cell. **(A)** Charts show fluctuations of the RNA concentrations in two different nucleoli of the same cell. On the right panel (**B**), a transmission light image of the studied cell is presented; arrows show two nucleoli where the RNA content was monitored. (**C**) Fluctuations of the RNA concentrations, in two separate nucleoli of the same cell; these data supplement charts shown in (**A**). Pearson correlation coefficients (r) between fluctuations of the RNA synthesis in different nucleoli of the same cell are 0.62, 0.87, 0.76 and 0.75, as indicated. The synchrony in changes of RNA production portrays extrinsic noise of gene expression caused by stochastic fluctuations of intracellular environment.

proteins concentrations, determines the sign. These fluctuations are due to both intrinsic and extrinsic noise in the production of r-proteins. The rRNA sequence transcribed by RNA Polymerase III was not included in our model to simplify the analysis.

The master equation reads:

$$\frac{dn_{RNA}}{dt} = -\text{sign}\left[n_{RNA} - \min\left\{n_p^i\right\}\right]kn_{RNA} - k_{ribo}n_{RNA}$$
$$n_p^{(i)} = n_p^0 \pm \Delta \cdot \text{rand}(0,1) \quad (1)$$

where n_{RNA} and n_{p} are the concentrations of RNA and all r-proteins, respectively, k is the RNA growth rate, k_{ribo} is the rate at which rRNA is exported from the nucleolus, Δ is the maximum deviation of r-protein concentration, n_{p}^0 is the initial concentration of r-proteins which is set to 1 in our modeling.

To model the optimal rates of rDNA expression, this equation is written with the assumption that it is energetically beneficial for a cell to suppress production of rRNA, compensating for any real-time variations in the concentration of any of the r-proteins, and thus preventing synthesis of excessive rRNA. Likewise, we assumed that rRNA production is boosted when its concentration is lower than the lowest concentration of r-proteins.

In our single-cell modeling Δ corresponds to measured concentration variations of nucleolar proteins. Fluctuations of rRNA output are adjusted in accordance with Δ, in order to minimize the expenditure of energy through the synthesis of rRNA and/or r-proteins. To generate the model, we assigned to n_{RNA} and n_{p}, relative concentrations of 1.0 arbitrary units (a.u.) at 0 min of observation and tuned k, k_{ribo} and Δt to achieve a maximal fit of the RNA fluctuations measured in different cell to the model.

By adjusting the values of all fitting parameters, we obtained model charts which were relatively close to the measured values of rRNA synthesis. The difference between the experimental measurements of RNA and the model chart did not exceed 15% (Fig. 5). Despite the non-concurrency of some extrema in the modeled and the experimental curves, which could be explained by a more detailed and sophisticated model of fluctuations, this simplified modeling of the "optimal" rDNA expression rates produced the oscillatory behavior of rRNA concentration with the frequency and the amplitude close to the experimental measurements (Fig. 5). The numerical modeling results show that the synthesis of rRNA and r-proteins can be well coordinated, irrespective of independent fluctuations in gene expression rates.

DISCUSSION

Synthesis of ribosomes is a vital biosynthetic activity, supplying the cells with protein-building macromolecular complexes. The cellular needs dictate synthesis of ~7,500 to 14,000 ribosomes per minute which consumes a vast amount of cellular energy [6a, 28]. The incredibly intense, complex and well-orchestrated process of ribosome biogenesis has been in the research spotlight for several decades, unraveling many cellular regulation mechanisms. In 2009, accomplishments in this field were highlighted by a Nobel Prize in chemistry awarded for the Xray-crystallography of ribosome [29].

The ribosome synthesis involves a large number of synthetic pathways. The molecular composition of each ribosome includes 79 r-proteins, three rRNA species derived from RNA polymerase I transcript and one rRNA sequence synthesized by RNA polymerase III. In addition, the cell has to synthesize approximately 200 proteins and several hundred small nucleolar RNA species, which transiently associate with rRNAs and r-proteins, and guide the formation of pre-ribosomal particles [7d, 22b]. Considering, the exceptionally high intensity of ribosome production, it is generally believed that in order to conserve resources, the cell should produce rRNA and r-protein ribosome constituents in equimolar concentrations, and thus coordinate their synthesis [6a]. Consistently, several gene regulation and signal transduction pathways that can either up-regulate or down-regulate all three classes of RNA polymerases in synchronous manner, have been identified [5b, 7, 30]. However, all known regulation mechanisms coordinating rRNA and r-protein synthesis involve a separation of the stimulus and the response in time and, therefore, cannot address rapid variations in the synthetic rates of biomolecules caused by stochastic factors. At the same time, the synthesis of ribosomal constituents in unbalanced amounts would impair the efficiency of cellular metabolism and thus would be a target of evolutionary selection.

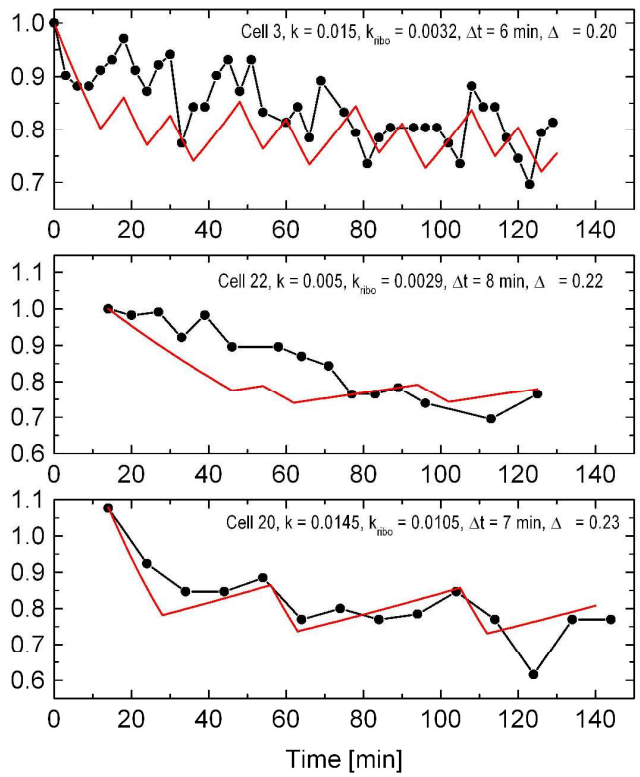

Figure 5: Fitting of numerically simulated and experimentally measured rates of rRNA synthesis. Time evolution of the RNA concentration governed by Eq.1 (red line), overlapped with experimentally measured RNA fluctuations patterns in the nucleoli of representative cells. Each chart indicates final coefficients for fitting of the numerical modeling charts (k - rate of rRNA synthesis, k_{ribo} – rate of rRNA export from nucleolus, Δt period of fluctuations and Δ deviation in concentrations of nucleolar proteins). We observed that numerically modeled optimal rates of rDNA expression are close to those experimentally measured.

Understanding how the rRNA synthesis is regulated requires quantitative monitoring at the level of individual cells. However, such studies are considerably challenging. Up-to-date two major approaches have been developed for monitoring RNA synthesis. One technique utilized fluorescent proteins for tagging of specific RNA sequences [15, 31], and another –molecular beacons, which are the single stranded nucleic acid probes that become fluorescent upon hybridization to the target molecule [32]. However, although the fluorescence techniques can be highly sensitive, selective and versatile, an inherent shortcoming is that either the expression or the delivery of exogenous fluorescence reporters into the cell can perturb cellular regulation [14]. Moreover, during imaging sessions, gradual bleaching of fluorescence signals and accumulation of the phototoxic damage in the studied cells may undermine the validity of obtained data. To our knowledge, fluorescence reporters have never been successfully applied for quantitative monitoring of rRNA synthesis, apparently due to high complexity of the rDNA system.

As a viable alternative to traditional techniques, presented here Raman spectroscopy approach permits to study the kinetics of rRNA synthesis in genetically unaltered and undamaged cells. For quantitative studies of the cellular processes, Raman spectroscopy provides several valuable benefits: (i) No labeling of cellular macromolecules is required, which reduces the experimental artifacts, (ii) Non-resonant excitation of Raman signal causes no measurable phototoxicity, allowing for a nondestructive monitoring of individual cells, (iii) High spatial resolution sufficient for a selective probing of distinct cellular organelles, (iv) High detection sensitivity and (v) Data acquisition rate is relatively fast, enabling the monitoring of macromolecular concentrations nearly in real-time [17a, 18, 33]. Notably, Raman spectroscopy can selectively analyze signals from major classes of macromolecules (i.e. proteins, RNA, DNA and lipids) which uniquely provides for quantitative monitoring of local molecular processes in specific organelles, in various physiological states of the cells [17a, 18, 33b, c].

In this study, an application of the Raman spectroscopy-BCA approach for monitoring of the nucleolus revealed surprisingly high and rapid fluctuations of the rRNA output. In systems biology, fluctuations of the RNA production have been traditionally viewed through the concept of extrinsic and intrinsic noises of gene expression, where the extrinsic noise is characterized by simultaneous changes in the activity of all identically regulated genes and the intrinsic noise is represented by random changes in the expression of any gene sequence [8a]. In this regards, separate rDNA clusters located in different nucleoli of the same cell offer a unique experimental system for identification of extrinsic component of the gene expression noise. Reported here synchronous changes in the output of rRNA in different nucleoli of the same cell nucleus are consistent with the definition of extrinsic noise caused by fluctuations in the amounts of soluble molecules, which regulate the rDNA expression. To understand significance of continuous fluctuations of RNA synthesis on biogenesis of ribosomes, it is important to consider that all three classes of RNA polymerase (i.e., RNA polymerase -I, -II and -III) are involved in the synthesis of rRNA and r-proteins. The extrinsic noise is inherently different for each type of RNA polymerase, which may compromise a coordinative production of ribosome constituents.

Frequent errors in translation or post-translation modifications of r-proteins can also hinder production of r-proteins and rRNA in balanced amounts. It has been reported that ~ 30% of r-proteins in HeLa cells are synthesized with structural defects and degraded [34]. In the study of Lam et. al., which utilized mass-spectrometry and fluorescence imaging to monitor assembly of pre-ribosomal particles, it was surprisingly found that r-proteins are synthesized in excessive amounts, with only a subset of them being utilized for ribosomal assembly [35]. Meanwhile, it has been reasoned that any disparity in the synthetic rates of various r-proteins and rRNA sequences would further increase the already high metabolic cost of ribosome production, first by excessive synthesis and then by ATP-dependent degradation of unused ribosome components [5b, 6a]. Intriguingly, while evolution theories postulate adjustment of gene expression levels to cellular needs [6b, 36], the efficiency of coordination of rRNAs and r-proteins productions is not clear yet.

Our study demonstrates advantages of a single-cell approach for quantitative monitoring of ribosome components. We believe that single-cell experimental models can provide valuable insight into fundamentals of cellular regulation.

Conclusions

Raman spectroscopy approach uniquely permits for label-free monitoring of rRNA synthesis in single cells. Using this technique we characterized the amplitude and frequency of fluctuations in the rates of rRNA synthesis, and demonstrated that they largely correspond to the extrinsic noise of gene expression. To our knowledge, it is a first quantitative characterization of real time-rates of specific genes expression in genetically unaltered cells. Intriguingly, numerical modeling indicates that the oscillatory pattern of rRNA synthesis may reflect an adaptation mechanism aimed at reduction of quantitative mismatches in the output of rRNA and r-proteins. We believe that modeling of rRNA and r-proteins synthesis may become a valuable tool for studies of gene networks coordination. Furthermore, a quantitative monitoring of rRNA synthesis by Raman microspectroscopy opens new research directions in computational biology and cell systems biology.

METHODS

Cell Culture and Drug Treatment

HeLa cells were obtained from ATTC (line CCL2) and were cultured in Advanced DMEM (Life Technologies) supplemented with 5% fetal bovine serum (Gibco), 1% penicillin/streptomycin and 3.7 g/liter NaHCO3 at 37^{o} C in a humidified atmosphere containing 5% CO2. During Raman microspectrometry data collection cells were maintained at 37^{o} C and 5% CO_2 in a Live-CellTM incubator (Pathology Devices) mounted at the microscope stage. For inhibition of RNA polymerase I cells were treated with actinomycin D (Sigma-Aldrich) (0.03 μg/ml for up to 4 h and 10 μg/ml for up to 1 h as designated) and for `inhibition of RNA polymerase II cells were treated with 5,6-dichloro-1-beta-D-ribofuranosylbenzimidazole (Sigma-Aldrich) (DRB) (50

μg/ml for up to 4 h) [37]. These transcription inhibitors were present in the cell culture medium during the Raman spectra acquisition. The data were collected in over fifty G1-phase cells.

Raman Microspectrometry: Instrumentation, Calibration and Data Analysis

This study employed Raman spectroscopy and Biomolecular Component Analysis (BCA) to identify concentrations of RNA and proteins in nucleolus, as described in our recent publications[17a]. The confocal Raman microspectrometer is based on an inverted Nikon TE200 microscope equipped with a He-Ne (Coherent, 632.8 nm) excitation laser, fiber-input MS3501i imaging monochromator/spectrograph (Solar TII), and Hamamatsu S9974 series CCD cooled down to -60°C. This configuration provides the Raman spectral measurement within the spectral range of 600-3000 cm^{-1}. The spectral resolution for the fixed diffraction grating position (wave number interval of 1210 cm^{-1}) was ~1.5 cm^{-1}. An excitation laser beam of ~30 mW power is focused onto the sample in a spot of ~ 0.8 μm using a 100× NA=1.3 Nikon oil-immersion objective lens. To enable signal acquisition in a confocal mode, a 100 μm pinhole was applied between the microscope output port and the optical fiber connected to the input of the spectrograph. The confocal parameter was estimated to be ~1.8 μm, as shown at the Fig. S4. Nucleoli were identified using transmission light. To ensure selective spectroscopic probing of nucleolus, relatively large nucleoli measuring no less than ~5 μm in diameter were selected and excitation laser beam was focused in the center of nucleolus. In control experiments, identification of the nucleoli by transmission light microscopy was validated with fluorescence imaging of nucleolar marker proteins, nucleolin and fibrillarin.

The accumulation time for Raman spectral measurements was 120 sec for all experiments. Raman spectroscopy studies did not produce any visible changes in cellular morphology, did not alter the cell cycle duration and showed no cytotoxicity by standard cell viability tests.

To ensure the absence of vibration, thermal drift or other motion in our system during experiments, we visually verified the XYZ position of the cell and studied nucleolus, before and after each measurement. To verify that detection sensitivity of Raman spectroscopy setup is stable we performed control time-lapse measurements of RNA and protein concentrations in nucleoli of formaldehyde fixed cells (Fig. S5). Measurements on the fixed cells also demonstrated homogeneity in the RNA and proteins concentrations in the central part of nucleolus [17a]. This result ensured that confident repetitive Raman measurements can be performed because variability from live cell/nucleolus motion is not substantial.

Experiments on Raman spectroscopy monitoring of two nucleoli in the same cell were performed as follows: Raman spectra were sequentially collected with 3-10 minute intervals between the acquisitions in each nucleolus. At each time point, spectrum was acquired for 2 minutes, after which excitation laser of Raman spectroscopy setup was rapidly refocused on another nucleolus in the cell. We estimate that intervals between acquisition of spectra in different nucleoli at corresponding time points were about 2 ¼ minutes.

All Raman spectra were preprocessed using background subtraction, Savitzky-Golay smoothing (2nd order of polynom and 13 points of smoothing) and baseline correction. Background elimination was performed by subtraction of the Raman spectra of incubation medium and background equalization of measured spectrum and corresponding BCA model spectrum. The measurements, performed on fixed cells, where biomolecular concentrations were "frozen", demonstrated, that experimental error of Raman spectra does not exceed 2-5% within the Raman shift range of 700-1700 cm^{-1} (Figure S5). Additional contribution to error is introduced by mismatch of model spectra (full set of weighted model components) and measured spectrum. Overall error is shown as error bars on experimental curves.

Measurements of molecular concentrations were performed at the characteristic vibrations: 1004 cm^{-1} - for proteins, 783- 813 cm^{-1} - for RNA/DNA and 1440 cm^{-1} - for lipids as described earlier[17a, 33b]. The concentration calibration and the specificity of detection were further verified on the Raman spectra of RNA –protein mixtures of known concentrations (Fig. S6). In additional control experiments, specificity of RNA and protein detection was verified in cells where either RNA or protein pools were selectively diminished. In these control experiments, the cells were permeabilized with 0.05 % of Triton X 100 for 5 min, and treated with either RNase (Roche Diagnostics) or proteinase K (Sigma Aldrich) for 10 min. We observed that RNase treatment results in strong reduction all RNA bands, while extraction of proteins leads to a significant decrease in all bands assigned to proteins (Figure S6), which further confirms molecular specificity of Raman measurements. Additional details on BCA accuracy and setup calibration are shown in Figures S7-S10.

For assessment of intranucleolar macromolecular information the BCA [17a] was applied to pre-processed Raman spectra. This method is based on an accurate spectral fit of a model spectrum - the linear summation of the weighted spectra of the basic components (Linear Combination Modeling (LCM) [17b, 38]), into a pre-processed Raman spectrum of nucleoli. The spectral weights (coefficients), which are varied during the fitting procedure, are considered as the specific contributions of the basic spectra into the resulting spectrum and relate directly to the concentrations of basic macromolecules. In our case LCM of the acquired Raman spectra was utilized for experimental evaluation of the local biomolecular composition in HeLa cells nucleoli by generating a model spectrum through a linear summation of weighted Raman spectra of the basic classes of organic bio-molecules, DNA, RNA, proteins, lipids, which make the largest contribution to nucleolar Raman spectrum [17a, 18]. In math terms it means to obtain a numerical value of the fractional fit contribution (weight, C_i) of each component, i, to Raman spectrum of measured nucleolar

domain (R_{total}): $R_{total} = C_1R_1+C_2R_2+C_3R_3+C_4R_4$, where R_i is Raman spectrum of i-component. The LCM algorithm was developed using a Matlab environment; it contains several cycles of the fitting the weighted model with the measured spectrum, including the separation of DNA and RNA contributions. More detailed description of BCA used in this study can be found in our previous publication [17a]. For initial step of BCA we used protein component (R_1), obtained from our previous studies of HeLa cell culture [17a] corresponding to 100 ml/mg of bovine serum albumin (C_1=1) equivalent of concentration. Then proteins spectra were defined more accurately during further steps of BCA. Preprocessed Raman spectra of extracted DNA, RNA, and lipid droplets from HeLa cells, calibrated to 20 mg/ml of calf thymus DNA, S. cerevisiae RNA and bovine heart lipid extract equivalents of concentration accordingly, were used as the reference spectra of the DNA, RNA and lipids components (R_i, i=2,3,4 with C_i=1, i=2,3,4). The correlation coefficients for data obtained in two nucleoli of the same cells were calculated using standard Microsoft Excel function.

Numerical Modeling

A fundamental theoretical and analytical apparatus for the analysis of the role of stochastic fluctuations of gene expression in gene regulation networks has been developed by Swain et al [9a]. Nevertheless, we implemented a simplified approach in order to isolate the principal mechanism of the observed oscillatory behavior. For numerical modeling of ribosomal genes system we assumed a negligible intrinsic noise for the synthesis of rRNA sequences by RNA polymerases I- and III, and r-proteins by RNA polymerase II based on both experimental findings as well as a known inverse correlation between rate of expression (exceptionally intense for ribosomal genes) and magnitude of intrinsic noise [8b]. Numerical modeling was performed in MATLAB environment (Release 2010a, MathWorks, Natick, MA, USA).

To generate charts on the Figure 5 were selected the following fitting parameters of the model: the initial concentration of rRNA (1.0 arbitrary units, a.u.), initial concentrations of proteins (1.0 a.u.), the time interval between triggering the variations of proteins concentrations (10 min), and the growth rate of rRNA (0.015 a.u./min).

Notes and references

[a] Institute for Lasers, Photonics and Biophotonics and the Department of Chemistry, University at Buffalo, the State University of New York, Buffalo, NY 14260

[b] Department of Biological Sciences, University at Buffalo, the State University of New York, Buffalo, NY 14260

[c] Department of Chemistry, Korea University, Seoul 136-701, Korea

 # Present Address: Aliaksandr Kachynski, Beckman Coulter, Inc. Life Science Division, 4862 Innovation Drive Fort Collins, CO 80525.

[†]These authors contributed equally

Corresponding Author

Correspondence to: pnprasad@acsu.buffalo.edu

Notes

The authors declare no competing financial interest.

ACKNOWLEDGMENT

We thank Dr K.M. Tramposch and Dr. H. Kutscher for helpful discussions. This work was supported in part by a grant from the Air Force Office of Scientific Research (Grants No. 1096313-1-58130 and No. FA95500610398)

.

ABBREVIATIONS

rRNA, ribosomal RNA; rDNA, ribosomal DNA; r-proteins, ribosomal proteins, BCA, biomolecular component analysis; LCM, Linear Combination Modeling.

REFERENCES

1. (a) I. Raska, K. Koberna, J. Malinsky, H. Fidlerova, M. Masata, The nucleolus and transcription of ribosomal genes. *Biol Cell* 2004, *96*. 579-594, DOI: DOI 10.1016/j.biolcel.2004.04.015; (b) I. Grummt, Wisely chosen paths--regulation of rRNA synthesis: delivered on 30 June 2010 at the 35th FEBS Congress in Gothenburg, Sweden. *FEBS J* 2010, *277*. 4626-39, DOI: 10.1111/j.1742-4658.2010.07892.x.

2. (a) H. Tschochner, E. Hurt, Pre-ribosomes on the road from the nucleolus to the cytoplasm. *Trends Cell Biol* 2003, *13*. 255-263, DOI: Doi 10.1016/S0962-8924(03)00054-0; (b) F. M. Boisvert, S. van Koningsbruggen, J. Navascues, A. I. Lamond, The multifunctional nucleolus. *Nat Rev Mol Cell Bio* 2007, *8*. 574-585, DOI: Doi 10.1038/Nrm2184.

3. (a) D. A. Jackson, A. B. Hassan, R. J. Errington, P. R. Cook, Visualization of Focal Sites of Transcription within Human Nuclei. *Embo J* 1993, *12*. 1059-1065; (b) I. Raska, P. J. Shaw, D. Cmarko, New insights into nucleolar architecture and activity. *Int Rev Cytol* 2006, *255*. 177-+, DOI: Doi 10.1016/S0074-7696(06)55004-1.

4. A. Pliss, K. Koberna, J. Vecerova, J. Malinsky, M. Masata, M. Fialova, I. Raska, R. Berezney, Spatio-temporal dynamics at rDNA foci: Global switching between DNA replication and transcription. *J Cell Biochem* 2005, *94*. 554-565, DOI: Doi 10.1002/Jcb.20317.

5. (a) M. Dundr, U. Hoffmann-Rohrer, Q. Y. Hu, I. Grummt, L. I. Rothblum, R. D. Phair, T. Misteli, A kinetic framework for a mammalian RNA polymerase in vivo. *Science* 2002, *298*. 1623-1626, DOI: DOI 10.1126/science.1076164; (b) S. Granneman, D. Tollervey, Building ribosomes: Even more expensive than expected? *Curr Biol* 2007, *17*. R415-R417, DOI: DOI 10.1016/j.cub.2007.04.011; (c) J. Malinsky, K. Koberna, J. Bednar, J. Stulik, I. Raska, Searching for active ribosomal genes in situ: light microscopy in light of the electron beam. *J Struct Biol* 2002, *140*. 227-31, DOI: S1047847702005749 [pii]; (d) A. K. Witkiewicz, N. Pliss, M. Kamma, S. Schnitt, H. J. Burstein, L. Harris, The effect of trastuzumab (Herceptin (R)) treatment on estrogen receptor status in patients with early stage HER2 positive breast cancer. *Lab Invest* 2005, *85*. 55a-55a.

6. (a) J. R. Warner, The economics of ribosome biosynthesis in yeast. *Trends Biochem Sci* 1999, *24*. 437-440; (b) D. Rudra, J. R. Warner, What better measure than ribosome synthesis? *Gene Dev* 2004, *18*. 2431-2436, DOI: Doi 10.1101/Gad.1254704.

7. (a) A. Laferte, E. Favry, A. Sentenac, M. Riva, C. Carles, S. Chedin, The transcriptional activity of RNA polymerase I is a key determinant for the level of all ribosome components. *Gene Dev* 2006, *20*. 2030-2040, DOI: Doi 10.1101/Gad.386106; (b) N. Gomez-Roman, Z. A. Felton-

Edkins, N. S. Kenneth, S. J. Goodfellow, D. Athineos, J. X. Zhang, B. A. Ramsbottom, F. Innes, T. Kantidakis, E. R. Kerr, J. Brodie, C. Grandori, R. J. White, Activation by c-Myc of transcription by RNA polymerases I, II and III. *Biochem Soc Symp* 2006. 141-154; (c) S. S. Johnson, C. Zhang, J. Fromm, I. M. Willis, D. L. Johnson, Mammalian Maf1 is a negative regulator of transcription by all three nuclear RNA polymerases. *Mol Cell* 2007, *26*. 367-379, DOI: DOI 10.1016/j.molcel.2007.03.021; (d) C. Mayer, I. Grummt, Ribosome biogenesis and cell growth: mTOR coordinates transcription by all three classes of nuclear RNA polymerases. *Oncogene* 2006, *25*. 6384-6391, DOI: DOI 10.1038/sj.onc.1209883; (e) M. S. Dai, H. Arnold, X. X. Sun, R. Sears, H. Lu, Inhibition of c-Myc activity by ribosomal protein L11. *Embo J* 2007, *26*. 3332-3345, DOI: DOI 10.1038/sj.emboj.7601776; (f) R. H. Pittman, M. T. Andrews, D. R. Setzer, A feedback loop coupling 5 S rRNA synthesis to accumulation of a ribosomal protein. *J Biol Chem* 1999, *274*. 33198-33201, DOI: DOI 10.1074/jbc.274.47.33198; (g) H. Lempiainen, D. Shore, Growth control and ribosome biogenesis. *Curr Opin Cell Biol* 2009, *21*. 855-63, DOI: S0955-0674(09)00158-6 [pii] 10.1016/j.ceb.2009.09.002.

8. (a) M. Kaern, T. C. Elston, W. J. Blake, J. J. Collins, Stochasticity in gene expression: From theories to phenotypes. *Nat Rev Genet* 2005, *6*. 451-464, DOI: Doi 10.1038/Nrg1615; (b) A. Raj, A. van Oudenaarden, Nature, nurture, or chance: stochastic gene expression and its consequences. *Cell* 2008, *135*. 216-26, DOI: S0092-8674(08)01243-9 [pii] 10.1016/j.cell.2008.09.050; (c) A. Eldar, M. B. Elowitz, Functional roles for noise in genetic circuits. *Nature* 2010, *467*. 167-173, DOI: Doi 10.1038/Nature09326; (d) G. Chalancon, C. N. J. Ravarani, S. Balaji, A. Martinez-Arias, L. Aravind, R. Jothi, M. M. Babu, Interplay between gene expression noise and regulatory network architecture. *Trends Genet* 2012, *28*. 221-232, DOI: DOI 10.1016/j.tig.2012.01.006.

9. (a) P. S. Swain, M. B. Elowitz, E. D. Siggia, Intrinsic and extrinsic contributions to stochasticity in gene expression. *P Natl Acad Sci USA* 2002, *99*. 12795-12800, DOI: DOI 10.1073/pnas.162041399; (b) M. B. Elowitz, A. J. Levine, E. D. Siggia, P. S. Swain, Stochastic gene expression in a single cell. *Science* 2002, *297*. 1183-1186, DOI: DOI 10.1126/science.1070919.

10. M. Kaern, T. C. Elston, W. J. Blake, J. J. Collins, Stochasticity in gene expression: from theories to phenotypes. *Nature reviews. Genetics* 2005, *6*. 451-64, DOI: 10.1038/nrg1615.

11. J. H. Levine, Y. H. Lin, M. B. Elowitz, Functional Roles of Pulsing in Genetic Circuits. *Science* 2013, *342*. 1193-1200, DOI: DOI 10.1126/science.1239999.

12. (a) L. Pelkmans, Using Cell-to-Cell Variability-A New Era in Molecular Biology. *Science* 2012, *336*. 425-426, DOI: DOI 10.1126/science.1222161; (b) J. M. Levsky, R. H. Singer, Gene expression and the myth of the average cell. *Trends Cell Biol* 2003, *13*. 4-6, DOI: S0962892402000028 [pii].

13. D. J. Wang, S. Bodovitz, Single cell analysis: the new frontier in 'omics'. *Trends Biotechnol* 2010, *28*. 281-290, DOI: DOI 10.1016/j.tibtech.2010.03.002.

14. A. Raj, A. van Oudenaarden, Single-molecule approaches to stochastic gene expression. *Annu Rev Biophys* 2009, *38*. 255-70, DOI: 10.1146/annurev.biophys.37.032807.125928.

15. S. Hocine, P. Raymond, D. Zenklusen, J. A. Chao, R. H. Singer, Single-molecule analysis of gene expression using two-color RNA labeling in live yeast. *Nat Methods* 2013, *10*. 119-121.

16. (a) C. Matthaus, B. Bird, M. Miljkovic, T. Chernenko, M. Romeo, M. Diem, Chapter 10: Infrared and Raman microscopy in cell biology. *Methods in cell biology* 2008, *89*. 275-308, DOI: 10.1016/S0091-679X(08)00610-9; (b) P. N. Prasad, *Introduction to biophotonics*. Wiley-Interscience: Hoboken, NJ, 2003; p xvii, 593 p., 8 p. of plates.

17. (a) A. N. Kuzmin, A. Pliss, A. V. Kachynski, Biomolecular component analysis of cultured cell nucleoli by Raman microspectrometry. *Journal of Raman Spectroscopy* 2013, *44*. 198-204, DOI: Doi 10.1002/Jrs.4173; (b) K. W. Short, S. Carpenter, J. P. Freyer, J. R. Mourant, Raman spectroscopy detects biochemical changes due to proliferation in mammalian cell cultures. *Biophys J* 2005, *88*. 4274-4288, DOI: DOI 10.1529/biophysj.103.038604; (c) A. Pliss, A. N. Kuzmin, A. V. Kachynski, P. N. Prasad, Nonlinear optical imaging and Raman microspectrometry of the cell nucleus throughout the cell cycle. *Biophysical journal* 2010, *99*. 3483-91, DOI: 10.1016/j.bpj.2010.06.069.

18. A. Pliss, A. N. Kuzmin, A. V. Kachynski, H. Jiang, Z. Hu, Y. Ren, J. Feng, P. N. Prasad, Nucleolar molecular signature of pluripotent stem cells. *Analytical chemistry* 2013, *85*. 3545-52, DOI: 10.1021/ac303806j.

19. S. Granneman, S. J. Baserga, Crosstalk in gene expression: coupling and co-regulation of rDNA transcription, pre-ribosome assembly and pre-rRNA processing. *Curr Opin Cell Biol* 2005, *17*. 281-286, DOI: DOI 10.1016/j.ceb.2005.04.001.

20. J. Klein, I. Grummt, Cell cycle-dependent regulation of RNA polymerase I transcription: the nucleolar transcription factor UBF is inactive in mitosis and early G1. *Proc Natl Acad Sci U S A* 1999, *96*. 6096-101.

21. S. Cooper, Rethinking synchronization of mammalian cells for cell cycle analysis. *Cell Mol Life Sci* 2003, *60*. 1099-1106, DOI: DOI 10.1007/s00018-003-2253-2.

22. (a) P. Roussel, C. Andre, L. Comai, D. HernandezVerdun, The rDNA transcription machinery is assembled during mitosis in active NORs and absent in inactive NORs. *J Cell Biol* 1996, *133*. 235-246, DOI: DOI 10.1083/jcb.133.2.235; (b) I. Grummt, Life on a planet of its own: regulation of RNA polymerase I transcription in the nucleolus. *Gene Dev* 2003, *17*. 1691-1702, DOI: Doi 10.1101/Gad.1098503r; (c) E. Muro, J. Gebrane-Younes, A. Jobart-Malfait, E. Louvet, P. Roussel, D. Hernandez-Verdun, The traffic of proteins between nucleolar organizer regions and prenucleolar bodies governs the assembly of the nucleolus at exit of mitosis. *Nucleus-Austin* 2010, *1*. 202-211; (d) D. Hernandez-Verdun, Assembly and disassembly of the nucleolus during the cell cycle. *Nucleus* 2011, *2*. 189-94, DOI: 10.4161/nucl.2.3.16246 1949-1034-2-3-6 [pii].

23. J. R. Pomerening, J. A. Ubersax, J. E. Ferrell, Rapid cycling and precocious termination of G1 phase in cells expressing CDK1AF. *Mol Biol Cell* 2008, *19*. 3426-3441, DOI: DOI 10.1091/mbc.E08-02-0172.

24. O. Bensaude, Inhibiting eukaryotic transcription: Which compound to choose? How to evaluate its activity? *Biochem Soc Symp* 2011, *2*. 103-108, DOI: 10.4161/trns.2.3.16172 2154-1264-2-3-2 [pii].

25. A. Popov, E. Smirnov, L. Kovacik, O. Raska, G. Hagen, L. Stixova, I. Raska, Duration of the first steps of the human rRNA processing. *Nucleus* 2013, *4*. 134-41, DOI: 23985 [pii] 10.4161/nucl.23985.

26. K. Burger, B. Muhl, T. Harasim, M. Rohrmoser, A. Malamoussi, M. Orban, M. Kellner, A. Gruber-Eber, E. Kremmer, M. Holzel, D. Eick, Chemotherapeutic Drugs Inhibit Ribosome Biogenesis at Various Levels. *Journal of Biological Chemistry* 2010, *285*. 12416-12425, DOI: DOI 10.1074/jbc.M109.074211.

27. K. Koberna, J. Malinsky, A. Pliss, M. Masata, J. Vecerova, M. Fialova, J. Bednar, I. Raska, Ribosomal genes in focus: new transcripts label the dense fibrillar components and form clusters indicative of "Christmas trees" in situ. *J Cell Biol* 2002, *157*. 743-748, DOI: DOI 10.1083/jcb.200202007.

28. (a) D. Gorlich, I. W. Mattaj, Protein kinesis - Nucleocytoplasmic transport. *Science* 1996, *271*. 1513-1518, DOI: DOI 10.1126/science.271.5255.1513; (b) J. D. Lewis, D. Tollervey, Like attracts like: Getting RNA processing together in the nucleus. *Science* 2000, *288*. 1385-1389.

29. (a) T. A. Steitz, From the Structure and Function of the Ribosome to New Antibiotics (Nobel Lecture). *Angew Chem Int Edit* 2010, *49*. 4381-4398, DOI: DOI 10.1002/anie.201000708; (b) V. Ramakrishnan, The Eukaryotic Ribosome. *Science* 2011, *331*. 681-682, DOI: DOI 10.1126/science.1202093; (c) A. Yonath, Polar Bears, Antibiotics, and the Evolving Ribosome (Nobel Lecture). *Angew Chem Int Edit* 2010, *49*. 4340-4354, DOI: DOI 10.1002/anie.201001297.

30. S. Fumagalli, A. Di Cara, A. Neb-Gulati, F. Natt, S. Schwemberger, J. Hall, G. F. Babcock, R. Bernardi, P. P. Pandolfi, G. Thomas, Absence of nucleolar disruption after impairment of 40S ribosome biogenesis reveals an rpL11-translation-dependent mechanism of p53 induction. *Nat Cell Biol* 2009, *11*. 501-8, DOI: ncb1858 [pii] 10.1038/ncb1858.

31. I. Golding, J. Paulsson, S. M. Zawilski, E. C. Cox, Real-time kinetics of gene activity in individual bacteria. *Cell* 2005, *123*. 1025-1036, DOI: DOI 10.1016/j.cell.2005.09.031.

32. S. Tyagi, F. R. Kramer, Molecular beacons: Probes that fluoresce upon hybridization. *Nat Biotechnol* 1996, *14*. 303-308, DOI: Doi 10.1038/Nbt0396-303.

33. (a) A. Pliss, A. N. Kuzmin, A. V. Kachynski, P. N. Prasad, Nonlinear Optical Imaging and Raman Microspectrometry of the Cell Nucleus throughout the Cell Cycle. *Biophys J* 2010, *99*. 3483-3491, DOI: S0006-3495(10)00839-8 [pii] 10.1016/j.bpj.2010.06.069; (b) A. N. Kuzmin, A. Pliss, P. N. Prasad, Changes in Biomolecular Profile in a Single Nucleolus during Cell Fixation. *Anal Chem* 2014, *86*. 10909-16, DOI: 10.1021/ac503172b; (c) N. Yadav, A. Pliss, A. Kuzmin, P. Rapali, L. Sun, P. Prasad, D. Chandra, Transformations of the macromolecular landscape at mitochondria during DNA-damage-induced apoptotic cell death. *Cell Death Dis* 2014, *5*. e1453, DOI: cddis2014405 [pii] 10.1038/cddis.2014.405.

34. U. Schubert, L. C. Anton, J. Gibbs, C. C. Norbury, J. W. Yewdell, J. R. Bennink, Rapid degradation of a large fraction of newly synthesized proteins by proteasomes. *Nature* 2000, *404*. 770-774.

35. Y. W. Lam, A. I. Lamond, M. Mann, J. S. Andersen, Analysis of nucleolar protein dynamics reveals the nuclear degradation of ribosomal proteins. *Curr Biol* 2007, *17*. 749-760, DOI: DOI 10.1016/j.cub.2007.03.064.

36. E. Dekel, U. Alon, Optimality and evolutionary tuning of the expression level of a protein. *Nature* 2005, *436*. 588-592, DOI: Doi 10.1038/Nature03842.

37. S. Huang, T. J. Deerinck, M. H. Ellisman, D. L. Spector, The perinucleolar compartment and transcription. *J Cell Biol* 1998, *143*. 35-47, DOI: Doi 10.1083/Jcb.143.1.35.

38. (a) R. J. Swain, S. J. Kemp, P. Goldstraw, T. D. Tetley, M. M. Stevens, Assessment of Cell Line Models of Primary Human Cells by Raman Spectral Phenotyping. *Biophys J* 2010, *98*. 1703-1711, DOI: DOI 10.1016/j.bpj.2009.12.4289; (b) K. E. Shafer-Peltier, A. S. Haka, M. Fitzmaurice, J. Crowe, J. Myles, R. R. Dasari, M. S. Feld, Raman microspectroscopic model of human breast tissue: implications for breast cancer diagnosis in vivo. *J Raman Spectrosc* 2002, *33*. 552-563, DOI: Doi 10.1002/Jrs.877; (c) H. P. Buschman, G. Deinum, J. T. Motz, M. Fitzmaurice, J. R. Kramer, A. van der Laarse, A. V. Bruschke, M. S. Feld, Raman microspectroscopy of human coronary atherosclerosis: Biochemical assessment of cellular and extracellular morphologic structures in situ. *Cardiovasc Pathol* 2001, *10*. 69-82, DOI: Doi 10.1016/S1054-8807(01)00064-3.

Biological Insight: Quantitative characterization of real-time rates of gene expression is essential for comprehensive understanding of cellular organization and functions. In our communication, we characterize kinetics of ribosomal RNA (rRNA) synthesis in nucleoli of single cells. Our studies revealed surprisingly high and rapid fluctuations of rRNA output. Based on experimental data, we performed a numerical modeling to elucidate coordination of different gene networks in process of ribosome biogenesis.

Technological Innovation: *We* introduced label-free vibrational Raman microspectrometry technique for quantitative monitoring of specific RNA synthesis. This approach enabled monitoring of rRNA production under physiological cell conditions and in the absence of exogenous markers.

Integration: Advanced biophotonics approach, described in our study, enables new research directions in cellular physiology and system cell biology.